

Theory of the Loschmidt echo and dynamical quantum phase transitions in disordered Fermi systems

Tuomas I. Vanhala and Teemu Ojanen

Computational Physics Laboratory, Physics Unit, Faculty of Engineering and Natural Sciences,
Tampere University, P.O. Box 692, FI-33014 Tampere, Finland and
Helsinki Institute of Physics P.O. Box 64, FI-00014, Finland

In this work we develop the theory of the Loschmidt echo and dynamical phase transitions in non-interacting strongly disordered Fermi systems after a quench. In finite systems the Loschmidt echo displays zeros in the complex time plane that depend on the random potential realization. Remarkably, the zeros coalesce to form a 2D manifold in the thermodynamic limit, atypical for 1D systems, crossing the real axis at a sharply-defined critical time. We show that this dynamical phase transition can be understood as a transition in the distribution function of the smallest eigenvalue of the Loschmidt matrix, and develop a finite-size scaling theory. Contrary to expectations, the notion of dynamical phase transitions in disordered systems becomes decoupled from the equilibrium Anderson localization transition. Our results highlight the striking qualitative differences of quench dynamics in disordered and non-disordered many-fermion systems.

Introduction— Equilibrium statistical physics is one of the most general theories in natural sciences - it has been successfully applied to a remarkably wide variety of systems between the smallest and the largest scales in the universe. Only recently, the advent of modern quantum simulators and digital quantum computers has enabled a detailed experimental access to coherent far-from-equilibrium quantum evolution [1–10]. One aspect of this that has recently stimulated enormous interest is the possibility for non-analytic behaviour generated by a sudden quench. This phenomenon, often discussed in terms of a many-body Loschmidt echo, has close analogies with equilibrium phase transitions which give rise to well-known non-analytic properties as a function of the control parameter driving the transition. In contrast, a so-called dynamical quantum phase transition, taking place at a critical time t_c , signifies a vanishing Loschmidt echo and an abrupt change in the temporal evolution [11]. The possibility of non-analytic evolution is in itself intriguing, however, the formal analogy with equilibrium criticality has launched a search for possible universal properties in far-from-equilibrium systems [11, 12].

In this work we establish the theory of Loschmidt echo and dynamical quantum phase transitions in non-interacting disordered many-fermion systems. We discover that the singular dynamics of disordered Fermi systems constitute a radical departure from the previously studied many-body quenches. We find that i) the temporal evolution of the studied system after a generic quench is accompanied by a vanishing Loschmidt echo after a finite time ii) the critical time, when the Loschmidt echo vanishes, becomes a deterministic non-fluctuating quantity in the thermodynamic limit iii) the Loschmidt echo remains strictly zero after the critical time iv) the qualitative behaviour of the Loschmidt echo does not depend on whether the quench crosses the equilibrium Anderson localization critical point or not. Many insights on dy-

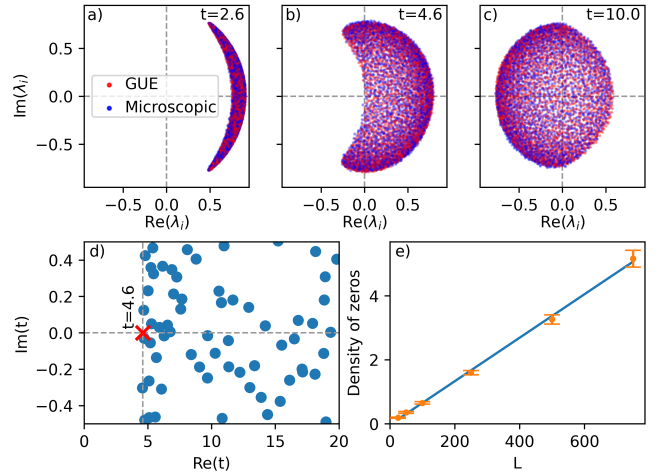


FIG. 1. Dynamical phase transition following a very strong sudden quench. a-c) Eigenvalues of the $M(t)$ -matrix for two different models, the GUE model and the microscopic model, which exhibit remarkable similarity. The dynamical phase transition occurs at the point $t = t_c$ where the boundary of the eigenvalue distribution crosses the origin. d) Loschmidt zeros for a single realization of the microscopic model. The red cross marks the dynamical phase transition point where the real axis intersects the boundary of the area with a finite zero-density. e) Scaling of the average density of zeros with system size L in the region $15 < \text{Re}(t) < 25$, $|\text{Im}(t)| < 0.2$. The datapoints were calculated with 100 realizations of the random potential for each L and the line is a linear regression.

namical phase transitions have been obtained from free-fermion systems and subsequently confirmed in a number of strongly-correlated systems. Thus, our present work provides a baseline to understand singular dynamics of even more complex disordered systems in the future.

Prototype model and quench protocol— We consider sudden quenches between two generic, non-interacting fermionic Hamiltonians H_0 and H_1 . The initial state $|\psi\rangle$

of the system at time $t = 0$ is taken to be an N_p -particle eigenstate of H_0 , which is then propagated by H_1 . Since both H_0 and H_1 are non-interacting, the state is a Slater determinant for all times. Collecting the N_p occupied orbitals in the initial state as columns of the matrix V , the evolved state $|\psi(t)\rangle$ is represented by a Slater determinant of the columns of $V(t) = \exp(-itH_1)V$, while the associated Loschmidt echo is given by [13]

$$Z(t) = \langle \psi | \psi(t) \rangle = \det(M(t)), \quad (1)$$

where the Loschmidt matrix $M(t)$ is defined as $M(t) = V^\dagger V(t)$. It is convenient to consider the echo in the eigenbasis of H_1 represented as $H_1 = U_1 E_1 U_1^\dagger$, where columns of U are the eigenstates of H_1 and E_1 is a diagonal matrix of the eigenenergies. The matrix $M(t)$ can be written as

$$M(t) = V^\dagger U_1 \exp(-itE_1) U_1^\dagger V, \quad (2)$$

and the echo is determined by the basis change matrix $V^\dagger U_1$ and the distribution of the energies E_1 .

As a prototype we consider a 1D Anderson model with a second quantized Hamiltonian of the form

$$H = J \sum_{i=1}^L (c_i^\dagger c_{i+1} + c_{i+1}^\dagger c_i) + \sum_{i=1}^L h_i c_i^\dagger c_i. \quad (3)$$

It is instructive to first consider the extreme quench where the initial Hamiltonian H_0 is free from disorder $h_i = 0, J = 1$ while the final Hamiltonian H_1 has no hopping $J = 0$ and h_i are drawn from a uniform distribution in the interval $[-h/2, h/2]$. We quench from an eigenstate of H_0 , randomly choosing N_p single-particle states to be occupied, and propagate with the Hamiltonian H_1 , whose spectrum is just given by the h_i . We always consider half-filling, $N_p = L/2$.

It is revealing to compare the microscopic model with an effective random matrix model where the initial Hamiltonian $H_0 = U_0 E_0 U_0^\dagger$ is drawn from the gaussian unitary ensemble (GUE). In this model it makes no difference what the eigenstates of H_1 are. This is because U_0 is distributed according to the circular unitary ensemble (CUE) and, by the invariance of the Haar measure, so is the overlap matrix $U_0^\dagger U_1$ regardless of what U_1 is. The matrix $V^\dagger U_1$ is thus just a randomly chosen collection of row vectors from a CUE random matrix regardless of U_1 . We still assume that the energies E_1 are the same as in the microscopic model, i.e. uniformly distributed in the interval $[-h/2, h/2]$.

Dynamical phase transitions are revealed by the zeros of $Z(t)$, termed the Loschmidt zeros, in the complex t -plane. A dynamical phase transition takes place at a critical time t_c , where the manifold of zeros intersects the real time axis. However, first we explore the Loschmidt echo by following the evolution of the eigenvalues of $M(t)$ and plotting them in the upper row of Fig. 1. As $Z(t)$ is the determinant of $M(t)$, zeros of $Z(t)$ appear at points

t where $M(t)$ has eigenvalue zero. We notice that the spectrum of $M(t)$ falls within a well-defined, bounded region at all times. After the appearance of the first zero eigenvalue, the spectrum of $M(t)$ encapsulates the origin at all times. This signifies a type of singular many-body dynamics where the Loschmidt echo vanishes for all times after first reaching zero and the only singularity of the rate function is at the critical time, similarly to the quench within the massless phase in the 2D Kitaev model [14]. Here we observe a certain universality, as the microscopic model and the GUE model produce essentially the same eigenvalue distribution.

We can now confirm the nature of the dynamical phase transition also by directly looking at the Loschmidt zeros which we locate using the cumulant method developed in [15]. We discuss the specialization of the method to the non-interacting case in the supplementary material [16]. In this case, as also clarified below, the Loschmidt zeros are organized as a 2D manifold. As seen in the lower left panel of Fig. 1, the zeros indeed cross the real time axis at the time t_c which coincides with the first appearance of zero eigenvalue of $M(t)$. The density of the Loschmidt zeros in the region $t > t_c$ increases proportionally to L , which we also verify numerically in Fig. 1e. The zeros thus form a two-dimensional manifold previously found in two-dimensional models [14], while one-dimensional models typically display lines of zeros [11]. Here, however, the zero manifold is two-dimensional for both the 1D microscopic model and for the random matrix model where the propagating Hamiltonian only enters through its eigenenergies, which are not directly related to its dimensionality.

Eigenvalue phase transition and scaling theory— In the case of extreme quenches between clean and non-hopping states discussed above, the eigenvalue distribution of $M(t)$ appears to have a sharp boundary and the critical time t_c is easily located by simply following the evolution of eigenvalues in the complex plane. However, for generic quenches this is not the case, as the boundary of the eigenvalue distribution in the thermodynamic limit may be difficult to determine from the finite set of eigenvalues calculated for some attainable system size L . Indeed, the question remains whether such a sharp boundary generally exists even in the thermodynamic limit. This is demonstrated in Fig. 2a for a quench starting from the ground state of Hamiltonian 3 at parameters ($h = 0, J = 1$) and propagated with ($h = 5, J = 1$).

To gain a quantitative understanding of the dynamical phase transitions in such cases, we consider ensembles of quenches for different realizations of the random potential. In Fig. 2b we plot the combined Loschmidt zeros for 100 systems of length $L = 500$. Although the zeros for a single system are very sparse, the ensemble reveals a sharp boundary where the zeros appear. From the viewpoint of the eigenvalues of $M(t)$, the same boundary is found by inspecting the density ρ_λ of eigenvalues close

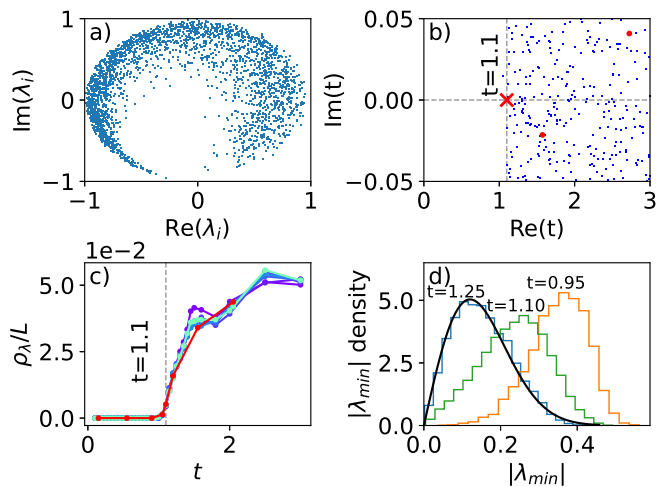


FIG. 2. Quenching from the ground state of the $(h = 0, J = 1)$ system to the $(h = 5, J = 1)$ system. a) Eigenvalues of $M(t)$ for a single potential realization in a system of size $L = 5000$ at the approximate critical time $t = 1.1$. b) Combined Loschmidt zeros for system size $L = 500$ and $N_s = 100$ potential realizations. The red dots highlight the zeros for one realization, showing their rarity. The red cross indicates the dynamical phase transition. c) The density of eigenvalues of $M(t)$ within a small disc of radius 0.05 around the origin averaged over a large number of potential realizations. The color coding for system sizes and the sample sizes are as in Fig. 3. d) Histogram of $N_s = 10000$ samples of $|\lambda_{min}|$ for different times in the $L = 500$ system. The black line is a Rayleigh distribution fitted to the data at $t = 1.25$.

to the origin averaged over the ensemble (see Fig. 2c). But is this sharp transition a property of the ensemble, or a property of an individual quench in the thermodynamic limit? If we could increase the system size sufficiently, would we obtain a sharp non-fluctuating critical time for an individual quench? To answer this question, we propose to study the distribution of $|\lambda_{min}|$, the absolute value of the smallest eigenvalue of $M(t)$. Assuming $M(t)$ is diagonalizable, this is the same as the smallest singular value of $M(t)$, which has also been studied in classical random matrix ensembles [17, 18].

Suppose now that a sharp boundary for the eigenvalue distribution of $M(t)$ exists in the thermodynamic limit. Then, for $t < t_c$, the distribution of $|\lambda_{min}|$ should become increasingly narrow with increasing L , and its mean $\langle |\lambda_{min}| \rangle$ should approach a finite value corresponding to the distance from the origin to the boundary of the eigenvalue distribution. For times $t > t_c$, on the other hand, both the mean and the standard deviation $\sigma(|\lambda_{min}|)$ of the distribution should scale to zero with increasing L . If we assume that the eigenvalues of $M(t)$ in the vicinity of the origin are drawn independently from some smooth distribution with local density ρ_λ , we find that the distribution of $|\lambda_{min}|$ converges to the Rayleigh form [16]

$$f(|\lambda_{min}|) = 2\pi r \rho_\lambda \exp(-\pi \rho_\lambda |\lambda_{min}|^2). \quad (4)$$

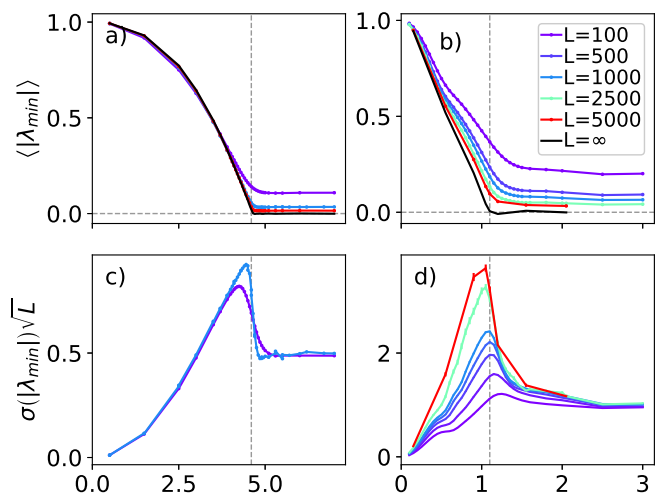


FIG. 3. Mean and scaled standard deviation of the distribution of $|\lambda_{min}|$ calculated for an ensemble of $N_s = 10000$ systems for $L \leq 500$ and $N_s = 1000$ for $L \geq 1000$. Panels a and c show the quench of the microscopic model also considered in Fig. 1, while panels b and d show the quench from the *ground state* of Hamiltonian 3 at $h = 0, J = 1$ propagated with the same Hamiltonian at parameters $h = 5, J = 1$. Black lines are calculated by a linear extrapolation in $1/\sqrt{L}$. The vertical dashed lines show the estimated critical time.

As it is expected that ρ_λ is proportional to L , the mean and standard deviation can both be calculated to be proportional to $1/\sqrt{L}$. We therefore expect a phase transition in the distribution of $|\lambda_{min}|$ at t_c where the scaling behaviour of $\langle |\lambda_{min}| \rangle$ as a function of L changes.

The distribution of λ_{min} is plotted in Fig. 2d for the $L = 500$ system around the critical time determined from the Loschmidt zeros. Indeed, we see the smallest eigenvalues reaching zero at $t \approx 1.1$ and the distribution undergoing a qualitative transition to a form that closely follows the Rayleigh distribution above critical times. That this is indeed a phase transition is demonstrated in Fig. 3 for two different quenches. In Fig 3a and Fig 3c we plot $\langle |\lambda_{min}| \rangle$ and $\sigma(|\lambda_{min}|)\sqrt{L}$ for the quench of the microscopic model also considered in Fig. 1. We observe a plateau in $\langle |\lambda_{min}| \rangle$ for $t \gtrsim t_c \approx 4.6$ consistently with the appearance of the Loschmidt zeros in Fig. 1. We have verified that $\langle |\lambda_{min}| \rangle$ scales as $1/\sqrt{L}$ in the large- t region. A phase transition is also clearly signalled by the jump in $\sigma(|\lambda_{min}|)\sqrt{L}$ observed at $t = t_c$. The apparent convergence of the curve for $\sigma(|\lambda_{min}|)\sqrt{L}$ indicates that the standard deviation scales as $1/\sqrt{L}$ for all times. This confirms that the eigenvalue distribution of $M(t)$ converges to a region with a well-defined boundary.

Fig. 3b and Fig. 3d show the corresponding data for a quench starting from the ground state of model 3 with $h = 0, J = 1$ and quenching to $h = 5, J = 1$. The behaviour of $\langle |\lambda_{min}| \rangle$ is similar with an initial decrease and a transition to a plateau where $\langle |\lambda_{min}| \rangle$ approaches zero with increasing L . The phase transition point can be esti-

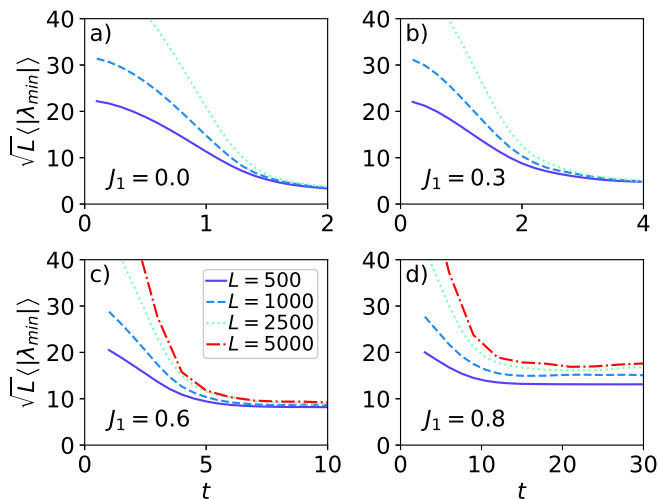


FIG. 4. Scaled mean of the distribution of $|\lambda_{min}|$ for quenches from the ground state of Hamiltonian 3. The system is quenched from $J = J_0 = 1, h = 5$ to $J = J_1, h = 5$ with the same random potential realization in the initial and final states. The panels show results for different J_1 . Ensemble sizes are as in Fig. 3.

mated from the extrapolated data as $t_c \approx 1.1$. The main difference to the previous quench is that $\sigma(|\lambda_{min}|)$ decreases slower than $1/\sqrt{L}$ for $t < t_c$, which is consistent with the qualitatively “fuzzier” boundary of the eigenvalue distribution compared to the quenches of Fig. 1. Nevertheless, for $t \gtrsim 1.1$ both the mean and the standard deviation scale to zero, indicating that $|\lambda_{min}| = 0$ for all realizations in the thermodynamic limit.

Strong and weak quenches— It has been widely observed that sudden quench through an equilibrium critical point in the parameter space typically results rich dynamics [19] and dynamical phase transitions compared to quenches confined to a same equilibrium phase. This property, though not without exceptions [20], is so generic that it has been proposed even as a diagnostic tool to investigate equilibrium phase boundaries. A remarkable feature of the transitions studied in this work is that they are not related to the underlying Anderson localization transitions. The model (3) exhibits Anderson localization for any disorder strength $h > 0$, and one might wonder if the DQPT is related to quenching from $h = 0$ to $h > 0$ or vice versa. This is not the case, as demonstrated in Fig. 4. Here the quench is between two points in the parameter space where the system is deep in the localized phase. However, it is evident that the scaling of $\langle |\lambda_{min}| \rangle$ with \sqrt{L} is different for early and late times, signifying an occurrence of a DQPT. We note that DQPTs appear also in the effective GUE model discussed above, which does not exhibit a localization transition.

We finally consider the difference between “weak” and “strong” quenches. If we let J_1 approach J_0 , the post-quench Hamiltonian approaches the initial Hamiltonian.

If the system had a gapped ground state, we would expect that the ground states of H_1 and H_0 also approach each other, and that any possible dynamical phase transition would eventually disappear. However, since there is no gap in the thermodynamic limit, this argument is not applicable. In fact, it seems that the DQPT appears also for small quenches of J but reaching the scaling limit requires larger system sizes, as seen in Fig. 3c and 3d.

Discussion and Summary— In this work we developed the theory of Loschmidt echo in strongly disordered non-interacting fermionic models after a quench. We showed that the zeros of the Loschmidt echo are best understood in terms of the eigenvalues of the Loschmidt matrix $M(t)$ defined in Eq. (1), and developed a scaling theory that links the discovered new type of singular many-body dynamics to phase transitions in the eigenvalue distribution of $M(t)$. Unexpectedly, we find that generic quenches lead to qualitatively similar DQPTs. Specifically, DQPTs appear also when performing quenches deep within the localized phase, which clearly rules out the idea that DQPTs could be employed to pinpoint equilibrium transitions in disordered systems. A similar DQPT was also found in a generic GUE random matrix model, which points to a rather universal phenomenon independent of details such as dimension as long as disorder is present in the quench power spectrum.

Our findings constitute a radical departure from the previous results in models exhibiting localization transitions. The bosonic Anderson model [21] and the fermionic Aubry-Andre model [22] were found to exhibit periodic Loschmidt zeros when quenched through the localization transition point, but not when quenched within the localized or delocalized phase. However, the crucial difference is that Ref. [22] considers a single fermion and Ref. [21] considers many bosons in the same single-particle state, while in our work we deal with generic fermionic Slater determinant states. Periodic dynamical phase transitions were also found in the many-body time evolution of the interacting Aubry-Andre model with system sizes up to $L = 100$ [23]. It would be interesting to revisit the Aubry-Andre model using the eigenvalues of the $M(t)$ -matrix and perform a scaling analysis to determine the type of the zero-manifolds as we have done here for the model with Anderson disorder.

Finally, from a methodological point of view, we expect the ideas developed in our work to be useful for treating many non-interacting fermionic models without translation invariance. Considering the eigenvalues of $M(t)$ is complementary to the recently developed cumulant method [15, 24] which has been successfully applied to various strongly-correlated systems in 1d and 2d. In the present work we developed a variant of the cumulant method to efficiently study large non-interacting but disordered models. We expect these ideas to stimulate further studies of the dynamics of disordered systems.

Acknowledgements— The authors acknowledge the

Academy of Finland project 331094 for support.

-
- [1] T. Tian, H.-X. Yang, L.-Y. Qiu, H.-Y. Liang, Y.-B. Yang, Y. Xu, and L.-M. Duan, Observation of Dynamical Quantum Phase Transitions with Correspondence in an Excited State Phase Diagram, *Phys. Rev. Lett.* **124**, 043001 (2020).
- [2] K. Xu, Z.-H. Sun, W. Liu, Y.-R. Zhang, H. Li, H. Dong, W. Ren, P. Zhang, F. Nori, D. Zheng, H. Fan, and H. Wang, Probing dynamical phase transitions with a superconducting quantum simulator, *Science Adv.* **6**, eaba4935 (2020).
- [3] A. Eckardt, Colloquium: Atomic quantum gases in periodically driven optical lattices, *Rev. Mod. Phys.* **89**, 011004 (2017).
- [4] N. Fläschner, D. Vogel, M. Tarnowski, B. S. Rem, D.-S. Lühmann, M. Heyl, J. C. Budich, L. Mathey, K. Sengstock, and C. Weitenberg, Observation of dynamical vortices after quenches in a system with topology, *Nat. Phys.* **14**, 265 (2018).
- [5] T. Fogarty, S. Deffner, T. Busch, and S. Campbell, Orthogonality catastrophe as a consequence of the quantum speed limit, *Physical Review Letters* **124**, 10.1103/physrevlett.124.110601 (2020).
- [6] X.-Y. Guo, C. Yang, Y. Zeng, Y. Peng, H.-K. Li, H. Deng, Y.-R. Jin, S. Chen, D. Zheng, and H. Fan, Observation of a Dynamical Quantum Phase Transition by a Superconducting Qubit Simulation, *Phys. Rev. Applied* **11**, 044080 (2019).
- [7] T. Tian, Y. Ke, L. Zhang, S. Lin, Z. Shi, P. Huang, C. Lee, and J. Du, Observation of dynamical phase transitions in a topological nanomechanical system, *Phys. Rev. B* **100**, 024310 (2019).
- [8] K. Wang, X. Qiu, L. Xiao, X. Zhan, Z. Bian, W. Yi, and P. Xue, Simulating Dynamic Quantum Phase Transitions in Photonic Quantum Walks, *Phys. Rev. Lett.* **122**, 020501 (2019).
- [9] J. Zhang, G. Pagano, P. W. Hess, A. Kyprianidis, P. Becker, H. Kaplan, A. V. Gorshkov, Z.-X. Gong, and C. Monroe, Observation of a many-body dynamical phase transition with a 53-qubit quantum simulator, *Nature* **551**, 601 (2017).
- [10] P. Jurcevic, H. Shen, P. Hauke, C. Maier, T. Brydges, C. Hempel, B. P. Lanyon, M. Heyl, R. Blatt, and C. F. Roos, Direct Observation of Dynamical Quantum Phase Transitions in an Interacting Many-Body System, *Phys. Rev. Lett.* **119**, 080501 (2017).
- [11] M. Heyl, Dynamical quantum phase transitions: a review, *Reports on Progress in Physics* **81**, 054001 (2018).
- [12] M. Heyl, Scaling and Universality at Dynamical Quantum Phase Transitions, *Phys. Rev. Lett.* **115**, 140602 (2015).
- [13] F. Plasser, M. Ruckebauer, S. Mai, M. Oppel, P. Marquetand, and L. González, Efficient and flexible computation of many-electron wave function overlaps, *Journal of chemical theory and computation* **12**, 1207 (2016).
- [14] M. Schmitt and S. Kehrein, Dynamical quantum phase transitions in the kitaev honeycomb model, *Phys. Rev. B* **92**, 075114 (2015).
- [15] S. Peotta, F. Brange, A. Deger, T. Ojanen, and C. Flindt, Determination of dynamical quantum phase transitions in strongly correlated many-body systems using loschmidt cumulants, *Phys. Rev. X* **11**, 041018 (2021).
- [16] See Supplemental Material at [URL will be inserted by publisher] for [give brief description of material].
- [17] T. Tao and V. Vu, Random matrices: the distribution of the smallest singular values, *Geometric and Functional Analysis* **20**, 260 (2010).
- [18] F. Benaych-Georges and R. R. Nadakuditi, The singular values and vectors of low rank perturbations of large rectangular random matrices, *Journal of Multivariate Analysis* **111**, 120 (2012).
- [19] A. Haldar, K. Mallayya, M. Heyl, F. Pollmann, M. Rigol, and A. Das, Signatures of quantum phase transitions after quenches in quantum chaotic one-dimensional systems, *Phys. Rev. X* **11**, 031062 (2021).
- [20] S. Vajna and B. Dóra, Disentangling dynamical phase transitions from equilibrium phase transitions, *Phys. Rev. B* **89**, 161105 (2014).
- [21] H. Yin, S. Chen, X. Gao, and P. Wang, Zeros of loschmidt echo in the presence of anderson localization, *Phys. Rev. A* **97**, 033624 (2018).
- [22] C. Yang, Y. Wang, P. Wang, X. Gao, and S. Chen, Dynamical signature of localization-delocalization transition in a one-dimensional incommensurate lattice, *Phys. Rev. B* **95**, 184201 (2017).
- [23] R. Modak and D. Rakshit, Many-body dynamical phase transition in a quasiperiodic potential, *Phys. Rev. B* **103**, 224310 (2021).
- [24] F. Brange, S. Peotta, C. Flindt, and T. Ojanen, Dynamical quantum phase transitions in strongly correlated two-dimensional spin lattices following a quench, *Phys. Rev. Research* **4**, 033032 (2022).

Expected distribution of minimal eigenvalue

To model the distribution of the minimal eigenvalue of the matrix $M(t)$ for $t > t_c$, we consider a small circle of radius R around the origin and assume that the eigenvalues within this circle are independently and uniformly distributed with density ρ_λ . The number of eigenvalues within the circle is thus $N = \pi R^2 \rho_\lambda$. The probability that all points are outside a smaller circle of radius r is

$$P(|\lambda_{min}| > r) = (1 - r^2/R^2)^N. \quad (5)$$

The cumulative distribution function for the scaled variable $|\lambda_{min}|/\sqrt{\rho_\lambda}$ is then

$$\begin{aligned} F(x) &= P(|\lambda_{min}|/\sqrt{\rho_\lambda} < x) = \\ &= P(|\lambda_{min}| < x/\sqrt{\rho_\lambda}) = 1 - P(|\lambda_{min}| > x/\sqrt{\rho_\lambda}) \\ &= 1 - \left(1 - \frac{\pi x^2}{\pi \rho_\lambda R^2}\right)^N = 1 - \left(1 - \frac{\pi x^2}{N}\right)^N. \end{aligned} \quad (6)$$

When the system size grows, we expect $\rho_\lambda \rightarrow \infty$ so that $N \rightarrow \infty$. The cumulative function then converges to

$$F(x) \rightarrow 1 - \exp(-\pi x^2). \quad (7)$$

The cumulative function of the Rayleigh distribution is usually written as

$$F_{Rayleigh}(x) = 1 - \exp(-x^2/(2\sigma^2)), \quad (8)$$

where σ is a scale parameter. Thus $|\lambda_{min}|\sqrt{\rho_\lambda}$ becomes Rayleigh distributed with scale parameter $\sigma = 1/\sqrt{2\pi}$, while the distribution of $|\lambda_{min}|$ becomes increasingly narrow as ρ_λ increases, and can be approximated by a Rayleigh distribution with the scale parameter $\sigma = 1/\sqrt{2\pi\rho_\lambda}$.

Specialization of the cumulant method for non-interacting systems

The cumulant method developed in [15] can be used to locate the Loschmidt zeros in the complex plane. In principle the method can be directly applied also to the non-interacting models discussed in this work. However, specializing the computation of the cumulants to the case of Slater determinant states naturally offers a huge numerical advantage, because it avoids handling general many-body state vectors.

The Loschmidt echo as a function of the imaginary time τ can be defined as

$$Z(\tau) = \langle \Psi | \exp(-\tau H_1) | \Psi \rangle, \quad (9)$$

where H_1 is the post-quench Hamiltonian and $|\Psi\rangle$ is taken to be some eigenstate of the pre-quench Hamiltonian H_0 . If H_0 is a non-interacting fermionic Hamiltonian, then the state $|\Psi\rangle$ is a Slater determinant of single-particle states. We collect the states to a tall matrix V so that each column is a single-particle eigenstate. If we also assume that H_1 is non-interacting, the state $|\Psi(\tau)\rangle = \exp(-\tau H_1) |\Psi\rangle$ is also always a Slater determinant where the single-particle states are time-developed by H_1 . Thus $|\Psi(\tau)\rangle$ is represented by the time-developed tall matrix $V(\tau) = \exp(-\tau H_1)V$.

The overlap of Slater determinants is given by the determinant of the overlap matrix [13],

$$Z(\tau) = \det(V^\dagger V(\tau)). \quad (10)$$

In the interacting case [15] the cumulants are calculated from the moments

$$\mu_n = \partial_\tau^n Z(\tau). \quad (11)$$

However, the first derivative of the determinant of a matrix $M(\tau) = V^\dagger V(\tau)$ is

$$\partial_\tau \det(M(\tau)) = \det(M(\tau)) \text{tr} (M(\tau)^{-1} \partial_\tau M(\tau)), \quad (12)$$

with successively more complicated formulas for higher derivatives. It is thus difficult to directly compute the moments as derivatives of the Z .

For the Slater determinant case we can instead start from the formula for the cumulants

$$\kappa_n = \partial_\tau^n \log(\det(M(\tau)))|_{\tau=\tau_0}, \quad (13)$$

which, for $n = 1$ becomes

$$\kappa_1 = \text{tr}(M(\tau)^{-1} \partial_\tau M(\tau))|_{\tau=\tau_0}. \quad (14)$$

Let us then define a matrix function $K'(\tau)$ such that

$$K'(\tau) = M(\tau)^{-1} \partial_\tau M(\tau), \quad (15)$$

or equivalently

$$\partial_\tau M(\tau) = M(\tau) K'(\tau). \quad (16)$$

We then have that $\kappa_n = \text{tr}(\partial_\tau^{n-1} K'(\tau))|_{\tau=\tau_0}$.

In the case of a single particle M would be a 1×1 matrix and we could just define $K(\tau) = \log(M(\tau)) = \log(Z(\tau))$, and $K'(\tau) = \partial_\tau K(\tau)$. K and M would then just be the cumulant and moment generating functions. However, we don't want to do so because the derivative of the matrix logarithm is again non-trivial, and we don't actually need to define $K(\tau)$. It's enough to have a well-defined $K'(\tau)$ which is not necessarily a derivative of a known function $K(\tau)$.

Now we can proceed as in the usual case to derive a formula that relates cumulants to moments. But now our moments and cumulants are matrices,

$$K'(\tau) = \sum_{n=1}^{\infty} K_n \frac{(\tau - \tau_0)^{n-1}}{(n-1)!}, \quad (17)$$

and

$$M(\tau) = \sum_{n=0}^{\infty} M_n \frac{(\tau - \tau_0)^n}{n!}. \quad (18)$$

Equating the coefficient of τ^{n-1} on both sides of equation 16 we get

$$\frac{M_n}{(n-1)!} = \sum_{k=1}^n M_{n-k} K_k \frac{1}{(k-1)!(n-k)!} = \frac{M_0 K_n}{(n-1)!} + \sum_{k=1}^{n-1} M_{n-k} K_k \frac{1}{(k-1)!(n-k)!} \quad (19)$$

which can be solved for K_n as

$$K_n = M_0^{-1} \left(M_n - \sum_{k=1}^{n-1} M_{n-k} K_k \frac{(n-1)!}{(k-1)!(n-k)!} \right) = M_0^{-1} \left(M_n - \sum_{k=1}^{n-1} \binom{n-1}{k-1} M_{n-k} K_k \right). \quad (20)$$

For the 1×1 case this again just reduces to the usual recursive formula for the cumulants in terms of the moments. In fact, it is the same formula, but it has to be remembered that the matrices do not necessarily commute.

Numerically, we first compute the moment matrices $M_n = V^\dagger \partial_\tau^n V(\tau)|_{\tau=\tau_0}$, and then use the recursive formula to get the cumulant matrices K_n . The cumulants κ_n are then found as the trace of the matrices K_n . Finding the zeros using the cumulants proceeds as in the interacting case [15].